



Published in final edited form as:

Acad Radiol. 2017 September ; 24(9): 1070–1078. doi:10.1016/j.acra.2017.02.006.

Improved estimation of coronary plaque and luminal attenuation using a vendor-specific model-based iterative reconstruction algorithm in contrast-enhanced CT coronary angiography

Yoshinori Funama^{1,*}, Daisuke Utsunomiya², Kenichiro Hirata², Katsuyuki Taguchi³, Takeshi Nakaura², Seitaro Oda², Masafumi Kidoh², Hideaki Yuki², and Yasuyuki Yamashita²

¹Department of Medical Physics, Faculty of Life Sciences, Kumamoto University, Kumamoto, Japan

²Department of Diagnostic Radiology, Faculty of Life Sciences, Kumamoto University, Kumamoto, Japan

³The Russell H. Morgan Department of Radiology and Radiological Science, The Johns Hopkins University School of Medicine, Baltimore, USA

Abstract

Rationale and Objectives—To investigate the stabilities of plaque attenuation and coronary lumen for different plaque types, stenotic degrees, lumen densities, and reconstruction methods using coronary vessel phantoms and the visualization of coronary plaques in clinical patients through coronary CT angiography.

Materials and Methods—We performed 320-detector volume scanning of vessel tubes with stenosis and a tube without stenosis using three types of plaque CT numbers. The stenotic degrees were 50% and 75%. Images were reconstructed with filtered back projection (FBP) and two types of iterative reconstructions (AIDR3D and FIRST), with stenotic CT number of approximately 40, 80, and 150 HU, respectively. In each case, the tubing of the coronary vessel was filled with diluted contrast material and distilled water to reach the target lumen CT numbers of approximately 350 HU and 450 HU, and 0 HU, respectively. Peak lumen and plaque CT numbers were measured to calculate the lumen–plaque contrast. In addition, we retrospectively evaluated the image quality with regard to coronary arterial lumen and the plaque in ten clinical patients on a four-point scale.

Results—At 50% stenosis, the plaque CT number with contrast enhancement increased for FBP and AIDR3D and the difference in the plaque CT number with and without contrast enhancement was 15–44 HU for FBP and 10–31 HU for AIDR3D. However, the plaque CT number for FIRST had a smaller variation and the difference with and without contrast enhancement was –12–8 HU.

Yoshinori Funama, Ph.D., Department of Medical Physics, Faculty of Life Sciences, Kumamoto University, 4-24-1 Kuhonji, Kumamoto 862-0976, Japan, funama@kumamoto-u.ac.jp, TEL +81-96-373-5455, FAX +81-96-373-5455.

Publisher's Disclaimer: This is a PDF file of an unedited manuscript that has been accepted for publication. As a service to our customers we are providing this early version of the manuscript. The manuscript will undergo copyediting, typesetting, and review of the resulting proof before it is published in its final citable form. Please note that during the production process errors may be discovered which could affect the content, and all legal disclaimers that apply to the journal pertain.

The visual evaluation score for the vessel lumen was 2.8 ± 0.6 , 3.5 ± 0.5 , and 3.7 ± 0.5 for FBP, AIDR3D, and FIRST, respectively.

Conclusion—The FIRST method controls the increase in plaque density and the lumen–plaque contrast. Consequently, it improves the visualization of coronary plaques in coronary CT angiography.

Keywords

Coronary plaque attenuation; lumen–plaque contrast; full statistical iterative reconstruction algorithm; coronary CT angiography

INTRODUCTION

Coronary CT angiography (CTA) with electrocardiogram (ECG) gating is an accurate non-invasive method to evaluate coronary artery disease (1–4). Potential applications of coronary CTA require high visualization of coronary arteries while maintaining radiation dose (5). In addition, coronary CTA raises concerns regarding evaluations of coronary stenosis and coronary plaque. Previous studies have associated high-risk plaque characteristics (e.g., positive remodeling, low CT number plaque, napkin-ring, sign and spotty calcium), as characterized by coronary CTA, with culprit lesions of the acute coronary syndrome (6–12). Therefore, diagnostic accuracy relies on knowledge of the plaque burden and high-risk plaque features. Regarding coronary plaque, CT number of coronary plaque varies with the increasing contrast enhancement of coronary lumen owing to partial volume effects, beam hardening, and plaque vascularity (13). Non-contrast CTA and dual-phase coronary CTA from non-contrast (first phase) and contrast enhancement (second phase) were previously applied to achieve accurate CT number of the coronary plaque (14–16).

Recently, an algorithm called “forward projected model-based iterative reconstruction solution” (FIRST) was developed as an iterative method for image reconstructions (17, 18). Unlike AIDR3D (19, 20), FIRST is an iterative reconstruction algorithm that models system optics, such as the detector element aperture, and improves image quality by iteratively minimizing a penalty-based cost function. FIRST can potentially improve the spatial resolution and CT number because it employs a more accurate model of X-ray physics (considering partial volume effects, beam hardening, etc.) than the former iterative method does, as well as an improved filtered back-projection (FBP) method.

Our study aims to investigate the stabilities of plaque attenuation and coronary lumen using coronary vessel phantoms and the visualization of coronary plaques in clinical patients through coronary CTA. Our phantom study involves different plaque combinations (soft, intermediate, and calcified), different stenosis (50% and 75%), different lumen densities (low and high lumen), and different reconstruction methods (FBP, AIDR3D, and FIRST).

MATERIALS AND METHODS

Our retrospective studies were approved by our institutional review board; informed patient consent for the analyses was waived.

Phantom Study

Phantom—For the coronary vessel models, we used three types of vessel tubes with stenosis and an acrylic tube without stenosis (Fuyo, Japan). The length and the inner lumen diameter of the coronary vessel models were 50.0 mm and 3.0 mm, respectively. To investigate cases with different stenotic CT numbers, we used stenotic degrees of 50% and 75% and the stenosis were composed of polystyrene, mono cast nylon, and acrylonitrile butadiene styrene copolymer. In our study, the 50% and 75% stenosis portions were used to mimic moderate and severe stenosis, respectively. We examined three types of plaque, namely, soft, intermediate, and calcified plaque; the stenotic CT number was approximately 40, 80, and 150 HU, respectively. In the case without stenosis, the tubing of the coronary vessel was controlled with diluted contrast material (iopamidol, Isovue 370; Bracco Diagnostics, Princeton, NJ) to reach the target lumen CT numbers of approximately 350 HU (low lumen diameter) and 450 HU (high lumen diameter). Then, we filled the same iodine density in each 50% or 75% stenotic lumen. In the case of simulated non-contrast-enhanced CT, the tubing of the coronary vessel was filled with distilled water. The coronary vessel model was fixed at the center of a water-filled polypropylene square container (26.7 cm wide, 36.3 cm long, and 17.8 cm high).

ECG-gated single-heartbeat CTA—We performed ECG-gated single-heartbeat coronary CTA, prospectively on a third-generation 320-row multidetector CT (MDCT) (Aquilion ONE Genesis; Toshiba Medical Systems, Otawara, Japan) (21–23). The scanner parameters were detector configuration, 320×0.5 mm; slice thickness, 0.5 mm; gantry rotation time, 0.275 sec; display field-of-view (FOV), 80×80 mm; and matrix, 512×512 . An ECG was acquired during volume scanning at a simulated 60-bpm heart rate signal using the demo mode for cardiac CT. The tube voltage and the current were 120 kVp and 360 mA, respectively. We set the exposure phase window (padding window) to 75% with the half-scan algorithm for 60 bpm. CT scanning was performed three times for each contrast enhancement scenario and each stenosis. Images were synchronously reconstructed from the ECG data using filtered back projection (FBP) and two types of iterative reconstruction algorithms (IR: AIDR3D, FIRST, Toshiba Medical Systems, Otawara, Japan) as well as a coronary standard kernel/filter (FC03) for FBP (24), the AIDR3D standard. Unlike FBP and AIDR3D, the FIRST method does not include kernels; rather, different parameters were set depending on the clinical application, e.g., body, bone, and lung. In our study, we used a clinically optimized cardiac parameter, “cardiac sharp,” for FIRST. FIRST is expected to provide accurate CT images because additional information concerning the focal spot size (optics model), photoelectric noise (statistical model), cone beam trajectory (cone beam model), and exact scan parameters (system model) are utilized in the iterative process. FIRST includes the forward imaging process that communicates the projection data domain and the image data domain. The agreement between the measured projection data and calculated (forward) projection data is maximized while the image-domain regularization controls the image noise and the spatial resolution. The FIRST “cardiac sharp” employs the regularization model focusing on the maximization of high-contrast spatial resolution rather than minimization of image noise. In contrast, the FIRST “body” emphasizes minimization of noise over maximization of spatial resolution. In order to accurately image small

structures such as coronary vessels, the FIRST “cardiac sharp” is considered to be appropriate.

Peak CT number and plaque CT number—To analyze the longitudinal lumen planes 0.5-mm multiplanar reformations (MPRs) were conducted (Fig. 1). The lumen CT number of pixels along the lumen diameter was measured, and a profile plot was obtained. To measure the profile curve, the rectangular region of interest (ROI) was set at 3.0 × 9.0 mm (Fig. 1). The measurements were repeated three times, and the mean value was calculated for each of the 72 image settings (three reconstruction methods × two lumen CT numbers × four cases, with [three plaque types] and without stenosis × three scans) for 50% stenosis portions; the same was calculated for the 72 image settings for 75% stenosis portions. The peak lumen CT number was obtained from the peak value of the profile curve with the iodine contrast portion, and the mean value was calculated from the three scans (Fig. 1). The plaque CT number was measured from the center of the plaque portions using the ROI of 3.0 × 0.8 mm (20 × 5 pixels) and the calculated mean value from the three scans (Fig. 1). The differences in the peak lumen CT number (*d-lumen CT num*) and the plaque CT number (*d-plaque CT num*) between the cases with (w/) and without (w/o) stenosis were calculated using the following equations, respectively:

$$d\text{-lumen CT num [HU]} = p\text{-lumen CT num w/o stenosis} - p\text{-lumen CT num w/ stenosis}$$

$$d\text{-plaque CT num [HU]} = p\text{-plaque CT num w/o stenosis} - p\text{-plaque CT num w/ stenosis}.$$

In addition, the lumen and plaque (lumen–plaque) contrast difference was calculated by subtracting the plaque CT number from the peak lumen CT number. The lumen–plaque contrast difference expressed the ratio of each lumen–plaque contrast to the lumen–plaque contrast with FBP.

Clinical study

Patients—Ten patients (three women and seven men; mean age 72 ± 13 years; range 49–87 years) were retrospectively evaluated in the clinical study. They were included according to the criteria of the patients undergoing both coronary CTA and conventional angiography between March and May 2016. Twelve stenotic lesions with non- or partially calcified plaques were detected using coronary CTA, and 50% or more stenosis was detected by conventional angiography.

Data acquisition—We used the following protocol with the same CT scanner as in the phantom study and prospective ECG-gating axial scans: 320 rows × 0.5-mm collimation, rotation time 0.275 sec, tube voltage 120 kVp, tube current 220–300 mA (automatic exposure control). Each patient received the beta blocker (6–12.5-mg landiolol hydrochloride) and sublingual nitroglycerin (0.3 mg) 5 min before data acquisition. The high-concentration iodinated contrast agent (Iopamiron 370 mgI/mL, Bayer, Osaka, Japan) was delivered via a 20-gauge intravenous catheter placed in an antecubital vein. The amount of contrast agent was tailored according to the patient body weight (300 mgI/kg), and it was injected over 12 s, immediately followed by a 40-mL saline flush at the same rate using a dual-head power injector (Dual Shot-Type GX7; Nemoto Kyorindo, Tokyo, Japan).

Synchronization between the flow of the contrast agent and the CT acquisition was achieved using a computer-assisted bolus tracking system. The trigger threshold was set at 200 HU for the ascending aortic region of interest. CT data acquisition commenced 6 s after the trigger.

Quantitative evaluation—Two radiologists in consensus measured the following parameters from axial source images of a circular region of interest: (i) mean CT number of the coronary arterial lumen and plaque at the stenosed segment; (ii) mean CT number of the perivascular fatty tissue; (iii) image noise, determined as the standard deviation of the CT number in the aorta. Then, the contrast-to-noise ratios (CNR) of the vessel and the plaque were calculated as follows:

$$CNR_{vessel} = (CT \text{ number of lumen} - CT \text{ number of perivascular fat}) / \text{image noise}$$

$$CNR_{plaque} = (CT \text{ number of plaque} - CT \text{ number of perivascular fat}) / \text{image noise}$$

Qualitative evaluation—All images were reviewed and interpreted on an image processing workstation (Zio station 2, Ziosoft, Tokyo, Japan) by two board-certified radiologists with 13 and 9 years of cardiac CT experience. The images included transverse source images, multiplanar reformations, and thin-slab (2-mm) maximum intensity projections at a window level of 200 HU and a width of 800 HU. The available images in this study were chosen because they were recommended for the interpretation of coronary CTA by the Society of Cardiovascular Computed Tomography Guidelines Committee (25). The images acquired with the three different reconstructions (FBP, AIDR3D, FIRST cardiac) were intermixed, and the reviewers were unaware of the reconstruction technique used and the identity of the patients. The reviewers in consensus evaluated the CT image quality with regard to coronary arterial lumen and plaques. The following four-point scale was used for the evaluation of coronary arterial lumen: 4 (excellent) = coronary stenosis is clearly depicted with accurate estimation of stenosis severity, providing useful information in clinical settings; 3 (good) = stenosis is depicted, but the degree of stenosis is over- or underestimated by 25%; 2 (fair) = stenosis is depicted, but the degree of stenosis is over- or underestimated by 50% or more; 1 (poor) = coronary stenosis cannot be identified. In the evaluation of the coronary plaques, the scale was as follows: 4 (excellent) = both the inner and outer margin of coronary plaque are clearly visualized; 3 (good) = the inner margin of coronary plaque is visualized, but the outer margin is partially unclear; 2 (fair) = the coronary plaque is present, but the outer margin of the coronary plaque is unclear; 1 (poor) = the coronary plaque cannot be identified.

Statistical analysis—We used the Kruskal–Wallis one-way analysis of variance (ANOVA) on ranks to compare the three datasets containing the lumen CT numbers and the plaque CT numbers from FBP, AIDR3D, and FIRST. When the overall differences were statistically significant, post-hoc analysis using a parametric- (the Tukey–Kramer test) and a non-parametric multiple comparison method (the Steel–Dwass test) was employed for the parametric data. Differences with $p < 0.05$ were considered statistically significant. Kruskal–Wallis one-way ANOVA was performed with a statistical software program (MedCalc, Mariakerke, Belgium). For the Steel–Dwass multiple comparison test, we used a statistics

software program (R, version 3.1.1, the R project for statistical computing; <http://www.r-project.org/>).

RESULTS

Phantom study

Lumen CT number—The lumen CT number without stenosis (0% stenosis) was 370.5 HU with FBP, 370.4 HU with AIDR3D, and 387.9 HU with FIRST for low lumen density; it was 451.7 HU with FBP, 453.6 HU with AIDR3D, and 464.7 HU with FIRST for high lumen density (Table 1). The lumen CT number using FIRST was slightly higher at 11–17 HU than with the other FBP and AIDR3D. In 50% and 75% stenosis, the lumen CT number with FIRST was much higher than with the other FBP and AIDR3D. The increasing value when using FIRST was 40 to 66 HU at 50% stenosis and 44 to 72 HU at 75% stenosis (Table 1). Figure 2 shows the difference in the lumen CT number with and without stenosis. At 50% stenosis, the lumen CT number with FBP and AIDR 3D exhibited lower values than that with FIRST. Consequently, the differences in the lumen CT number with and without stenosis were large, from –32 HU to –68 HU with FBP and from –8.0 HU to –76 HU with AIDR3D. In contrast, the difference with and without stenosis for FIRST was from –1.3 HU to –24 HU and smaller than those using the other methods ($p < 0.05$, FBP; $p < 0.05$, AIDR3D). At 75% stenosis, the lumen CT number was substantially lower than that without stenosis. In addition, the values were larger than those with 50% stenosis. The difference with and without stenosis ranged from –141 HU to –196 HU with FBP, from –152 HU to –200 HU with AIDR3D, and from –115 HU to –151 with FIRST.

Plaque CT number—At 50% stenosis, the plaque CT number without contrast enhancement (non-contrast enhancement) was almost the same irrespective of the reconstruction method applied (Table 2). However, the plaque CT number with contrast enhancement was greater for FBP and AIDR3D, and the difference in the plaque CT number with and without contrast enhancement was 15 to 44 HU for FBP and 10 to 31 HU for AIDR3D (Table 2, Fig. 3). Compared with FBP and AIDR3D, the plaque CT number with contrast enhancement was slightly different with FIRST, and the difference ranged from –12 to 8 HU for a smaller variation of the plaque CT number ($p < 0.05$, FBP; $p < 0.05$, AIDR3D [Fig. 2]). At 75% stenosis, the difference in the plaque CT number with and without contrast enhancement was smaller than at 50% stenosis in FBP and AIDR3D (from –2 to 13 HU with FBP, from –5 to 18 HU with AIDR3D). However, the plaque CT number with FIRST remained almost constant between 50% and 75% stenosis. Figure 4 shows the profile curve of lumen CT number with 75% stenosis obtained from FBP, AIDR3D, and FIRST images. The FIRST image gave a narrower profile curve than the other images. The FIRST image data indicated a higher CT number in the iodine lumen portion and a decreased value for the plaque portion compared with FBP and AIDR3D. Table 3 shows the lumen–plaque contrast ratio with FBP, AIDR3D, and FIRST to that of FBP. The FIRST method improved the lumen–plaque contrast, and the ratio was 1.2–1.4 times at 50% stenosis and 1.4–1.6 times at 75% higher compared with the lumen–plaque contrast with FBP.

Clinical study

Quantitative evaluation—The CNR_{vessel} was 8.5 ± 3.2 , 14.4 ± 4.9 , and 19.8 ± 7.7 for FBP, AIDR3D, and FIRST, respectively. The CNR_{vessel} for FIRST was highest among the three methods, although the difference was not significant between AIDR3D and FIRST (Table 4). The CNR_{plaque} was 3.5 ± 1.5 , 6.1 ± 3.0 , and 8.8 ± 4.9 for FBP, AIDR3D, and FIRST, respectively. There was a significant difference in the CNR_{plaque} between the FBP and FIRST reconstructions (Table 4).

Qualitative evaluation—Figure 5 shows the clinical images obtained with FBP, AIDR3D, and FIRST. The visual evaluation score for the vessel lumen was 2.8 ± 0.6 , 3.5 ± 0.5 , and 3.7 ± 0.5 for FBP, AIDR3D, and FIRST, respectively. There were significant differences between the reconstruction methods except for AIDR3D vs FIRST (Table 5).

DISCUSSION

In general, iterative reconstruction can effectively reduce the image noise, leading to low-dose scanning (26–29). However, the problem of plastic/blotchy image appearance is an issue for statistical iterative reconstructions, and it is unclear whether the spatial resolution of small structures with model-based iterative reconstructions should be preserved. The new model-based iterative reconstruction method FIRST has balanced projection-data and volume-data domains and focuses on improving spatial resolution. Our results show the usefulness of FIRST for assessing coronary arteries. In small vessels such as coronary arteries, the partial volume effect and spatial resolution are insufficient, and the vessel pixel value might be biased from the true value. Compared with the FBP and AIDR3D, FIRST, which models the system optics, can reduce the degradation of the spatial resolution.

At 50% and 75% stenosis, FIRST suppresses the decreasing lumen CT number, in contrast to FBP and AIDR3D. The lumen CT number with 50% stenosis is lower than that without stenosis with FBP and AIDR3D. In contrast, with FIRST, the lumen CT number with and without stenosis is almost the same. At 75% stenosis, the lumen CT number is lowered in all reconstruction methods because the plaque area is wider and the iodine contrast area is restricted more than that in the lumen with 50% stenosis. However, the FIRST method shows a lower reduction in the lumen CT number than FBP and AIDR3D.

Unlike FIRST, the plaque CT number with contrast enhancement exhibits a greater increase with the FBP and AIDR3D methods than that with non-contrast enhancement. In particular, the increase ratio for soft plaque is higher than those for intermediate and calcified plaque. This is because the CT number for soft plaque is approximately 40 HU and is highly affected by iodinated lumen CT number (350 HU or 450 HU). Cademartiri et al. (30) investigated the increasing plaque CT number and reported that the lumen CT number significantly affects the measured plaque CT number, when using FBP; the plaque CT number increases with the lumen CT number. In our study, FIRST controls the plaque CT number and the value slightly decreases instead of increasing. At 75% stenosis, the plaque area increases more than the iodine portion area in the lumen, and the increasing plaque CT number is lower than that of 50% stenosis in FBP and AIDR3D. The FIRST method tends to decrease the plaque CT number in both cases (50% and 75% stenosis) compared with non-

contrast enhancement. This phenomenon may be owing to the effect of used parameter of cardiac-sharp in FIRST and the slight undershoot effect appears to preserve the lumen edge (Fig. 4).

The lumen–plaque contrast improves with the FIRST method than with FBP and AIDR3D in a clinical situation. We evaluate the effects of different reconstruction techniques on the image quality of the coronary lumen and plaque in clinical settings. FIRST demonstrates the best objective and subjective image quality, and our phantom study might support the clinical results. In the CNR vessel and the CNR plaque, there are no significant differences between AIDR3D and FIRST reconstructions. We propose that this may be because the number of our clinical subjects is small (only 12 lesions in 10 patients). Our visual evaluation results show that FIRST is significantly superior to FBP and AIDR3D for plaque visualization. We believe the mathematical characteristics of FIRST reconstruction improved the objective as well as subjective image quality in the clinical study, although the number of patients was small. Clinical image analysis using a larger number of patients is now underway in our laboratory. In this study, we focused on differences in the visualization of coronary arterial lumen and plaque using different reconstruction techniques, including FBP, AIDR3D, and FIRST, compared with the conventional radiation dose. We did not evaluate the effects of FIRST on radiation dose reduction. Further studies should be conducted to compare the objective and subjective image quality of low-dose FIRST images with that of FBP and AIDR3D images.

Accurate plaque CT numbers are required both for contrast-enhanced and non-contrast-enhanced images because the evaluation of high-risk plaque including soft plaque (low-attenuation plaque) features improves the diagnostic accuracy of acute coronary syndrome. Ferencik et al. (8) showed that when observing the high-risk plaque features of the worst lesion, patients with acute coronary syndrome had a larger volume of plaque with < 30 HU and < 60 HU, a higher remodeling index, and longer plaques. In addition, the proportion of lesions with positive remodeling and spotty calcium was higher in those patients as well. Furthermore, Dalager et al. (13) indicated significant increases in the HU-values in non-calcified plaque by increasing the luminal density. The Rule Out Myocardial Infarction/ Ischemia Using Computer Assisted Tomography (ROMICAT) trial showed that the sensitivity of obstructive coronary stenosis for acute coronary syndrome was limited to 77% (31). Therefore, characterization of a coronary plaque causing mild-to-moderate stenosis is a clinically important role of coronary CTA for appropriate patient management. The CT number of a soft plaque (unstable plaque) is approximately 40 HU (32) and that of a fibrous plaque (stable plaque) is 80–100 HU (7). Our phantom study results (50% stenosis model with 40-HU plaque) suggested that the non-calcified plaque changed subtype from soft/lipid-rich to fibrotic with FBP and AIDR3D. On the other hand, quantitative measurements with FIRST provided more accurate estimation of plaque attenuation, and we posit that FIRST can help avoid mischaracterization of coronary plaques.

The method presented in this study presents some limitations. First, this method does not consider motion in the coronary vessel models; artifacts derived from the heartbeat are not reproduced by our model. The second limitation is that we use the standard coronary kernel (FC03) for FBP, AIDR3D, and the optimized cardiac parameter (cardiac sharp) for FIRST,

and we did not investigate the other parameters. Third, in image evaluation, we applied so that to unaware the reconstruction techniques in reviewing. However, reviewers might suppose the reconstruction method from the slight differences of image characteristics. Finally, we used a lumen diameter of 3.0 mm including 50% and 75% stenosis in our phantom study. When the lumen diameter decreases, the variations in the lumen and plaque CT numbers are uncertain, especially using the FIRST method. We need to study the relation between lumen–plaque contrast, its vitalization, and the lumen diameter in a clinical situation.

In conclusion, the FIRST method controls the increases in plaque densities and the lumen–plaque contrast and consequently improves the visualization of coronary plaques compared with FBP and AIDR3D on coronary CTA.

Acknowledgments

We are grateful to Satoko Maesaki, Toshiba Medical Systems for advices on technical aspects of this study.

References

1. Oncel D, Oncel G, Tastan A, Tamci B. Evaluation of coronary stent patency and in-stent restenosis with dual-source CT coronary angiography without heart rate control. *AJR American journal of roentgenology*. 2008; 191(1):56–63. [PubMed: 18562725]
2. Mollet NR, Cademartiri F, van Mieghem CA, et al. High-resolution spiral computed tomography coronary angiography in patients referred for diagnostic conventional coronary angiography. *Circulation*. 2005; 112(15):2318–23. [PubMed: 16203914]
3. Leschka S, Alkadhi H, Plass A, et al. Accuracy of MSCT coronary angiography with 64-slice technology: first experience. *Eur Heart J*. 2005; 26(15):1482–7. [PubMed: 15840624]
4. Miller JM, Rochitte CE, Dewey M, et al. Diagnostic performance of coronary angiography by 64-row CT. *N Engl J Med*. 2008; 359(22):2324–36. [PubMed: 19038879]
5. Chen MY, Shanbhag SM, Arai AE. Submillisievert median radiation dose for coronary angiography with a second-generation 320-detector row CT scanner in 107 consecutive patients. *Radiology*. 2013; 267(1):76–85. [PubMed: 23340461]
6. Cury RC, Abbara S, Achenbach S, et al. CAD-RADS(TM) Coronary Artery Disease - Reporting and Data System. An expert consensus document of the Society of Cardiovascular Computed Tomography (SCCT), the American College of Radiology (ACR) and the North American Society for Cardiovascular Imaging (NASCI). Endorsed by the American College of Cardiology. *J Cardiovasc Comput Tomogr*. 2016; 10(4):269–81. [PubMed: 27318587]
7. Utsunomiya D, Fukunaga T, Oda S, et al. Multidetector computed tomography evaluation of coronary plaque morphology in patients with stable angina. *Heart Vessels*. 2011; 26(4):392–8. [PubMed: 21132306]
8. Ferencik M, Mayrhofer T, Puchner SB, et al. Computed tomography-based high-risk coronary plaque score to predict acute coronary syndrome among patients with acute chest pain--Results from the ROMICAT II trial. *J Cardiovasc Comput Tomogr*. 2015; 9(6):538–45. [PubMed: 26229036]
9. Fuchs TA, Fiechter M, Gebhard C, et al. CT coronary angiography: impact of adapted statistical iterative reconstruction (ASIR) on coronary stenosis and plaque composition analysis. *The international journal of cardiovascular imaging*. 2013; 29(3):719–24. [PubMed: 23053859]
10. Precht H, Kitslaar PH, Broersen A, et al. Influence of Adaptive Statistical Iterative Reconstruction on coronary plaque analysis in coronary computed tomography angiography. *J Cardiovasc Comput Tomogr*. 2016; 10(6):507–16.

11. Puchner SB, Ferencik M, Karolyi M, et al. The effect of iterative image reconstruction algorithms on the feasibility of automated plaque assessment in coronary CT angiography. *The international journal of cardiovascular imaging*. 2013; 29(8):1879–88. [PubMed: 23990390]
12. Puchner SB, Ferencik M, Maurovich-Horvat P, et al. Iterative image reconstruction algorithms in coronary CT angiography improve the detection of lipid-core plaque—a comparison with histology. *European radiology*. 2015; 25(1):15–23. [PubMed: 25182630]
13. Dalager MG, Bottcher M, Andersen G, et al. Impact of luminal density on plaque classification by CT coronary angiography. *The international journal of cardiovascular imaging*. 2011; 27(4):593–600. [PubMed: 20820922]
14. Yoshioka K, Tanaka R, Muranaka K, et al. Subtraction coronary CT angiography using second-generation 320-detector row CT. *The international journal of cardiovascular imaging*. 2015; 31(Suppl 1):51–8. [PubMed: 25721727]
15. Kidoh M, Utsunomiya D, Oda S, et al. Evaluation of the Effect of Intracoronary Attenuation on Coronary Plaque Measurements Using a Dual-phase Coronary CT Angiography Technique on a 320-row CT Scanner--In Vivo Validation Study. *Acad Radiol*. 2016; 23(3):315–20. [PubMed: 26777592]
16. Kidoh M, Utsunomiya D, Oda S, et al. Optimized subtraction coronary CT angiography protocol for clinical use with short breath-holding time-initial experience. *Acad Radiol*. 2015; 22(1):117–20. [PubMed: 25481519]
17. Nishiyama Y, Tada K, Nishiyama Y, et al. Effect of the forward-projected model-based iterative reconstruction solution algorithm on image quality and radiation dose in pediatric cardiac computed tomography. *Pediatr Radiol*. 2016
18. Yasaka K, Kamiya K, Irie R, Maeda E, Sato J, Ohtomo K. Metal artefact reduction for patients with metallic dental fillings in helical neck computed tomography: comparison of adaptive iterative dose reduction 3D (AIDR 3D), forward-projected model-based iterative reconstruction solution (FIRST) and AIDR 3D with single-energy metal artefact reduction (SEMAR). *Dentomaxillofac Radiol*. 2016; 45(7):20160114. [PubMed: 27268082]
19. Gervaise A, Osemont B, Lecocq S, et al. CT image quality improvement using Adaptive Iterative Dose Reduction with wide-volume acquisition on 320-detector CT. *European radiology*. 2012; 22(2):295–301. [PubMed: 21927791]
20. Chen MY, Steigner ML, Leung SW, et al. Simulated 50 % radiation dose reduction in coronary CT angiography using adaptive iterative dose reduction in three-dimensions (AIDR3D). *The international journal of cardiovascular imaging*. 2013; 29(5):1167–75. [PubMed: 23404384]
21. Einstein AJ, Elliston CD, Arai AE, et al. Radiation dose from single-heartbeat coronary CT angiography performed with a 320-detector row volume scanner. *Radiology*. 2010; 254(3):698–706. [PubMed: 20177085]
22. Nikolic B, Khosa F, Lin PJ, et al. Absorbed radiation dose in radiosensitive organs during coronary CT angiography using 320-MDCT: effect of maximum tube voltage and heart rate variations. *AJR American journal of roentgenology*. 2010; 195(6):1347–54. [PubMed: 21098194]
23. Qin J, Liu LY, Fang Y, et al. 320-detector CT coronary angiography with prospective and retrospective electrocardiogram gating in a single heartbeat: comparison of image quality and radiation dose. *The British journal of radiology*. 2012; 85(1015):945–51. [PubMed: 22745204]
24. Kitagawa K, George RT, Arbab-Zadeh A, Lima JA, Lardo AC. Characterization and correction of beam-hardening artifacts during dynamic volume CT assessment of myocardial perfusion. *Radiology*. 2010; 256(1):111–8. [PubMed: 20574089]
25. Leipsic J, Abbara S, Achenbach S, et al. SCCT guidelines for the interpretation and reporting of coronary CT angiography: a report of the Society of Cardiovascular Computed Tomography Guidelines Committee. *J Cardiovasc Comput Tomogr*. 2014; 8(5):342–58. [PubMed: 25301040]
26. Husarik DB, Marin D, Samei E, et al. Radiation dose reduction in abdominal computed tomography during the late hepatic arterial phase using a model-based iterative reconstruction algorithm: how low can we go? *Invest Radiol*. 2012; 47(8):468–74. [PubMed: 22717881]
27. Scheffel H, Stolzmann P, Schlett CL, et al. Coronary artery plaques: cardiac CT with model-based and adaptive-statistical iterative reconstruction technique. *Eur J Radiol*. 2012; 81(3):e363–9. [PubMed: 22197733]

28. Funama Y, Taguchi K, Utsunomiya D, et al. Image quality assessment of an iterative reconstruction algorithm applied to abdominal CT imaging. *Phys Med.* 2014; 30(4):527–34. [PubMed: 24662097]
29. Leipsic J, Labounty TM, Heilbron B, et al. Adaptive statistical iterative reconstruction: assessment of image noise and image quality in coronary CT angiography. *AJR American journal of roentgenology.* 2010; 195(3):649–54. [PubMed: 20729442]
30. Cademartiri F, Mollet NR, Runza G, et al. Influence of intracoronary attenuation on coronary plaque measurements using multislice computed tomography: observations in an ex vivo model of coronary computed tomography angiography. *European radiology.* 2005; 15(7):1426–31. [PubMed: 15750815]
31. Hoffmann U, Bamberg F, Chae CU, et al. Coronary computed tomography angiography for early triage of patients with acute chest pain: the ROMICAT (Rule Out Myocardial Infarction using Computer Assisted Tomography) trial. *J Am Coll Cardiol.* 2009; 53(18):1642–50. [PubMed: 19406338]
32. Yamamoto H, Kitagawa T, Ohashi N, et al. Noncalcified atherosclerotic lesions with vulnerable characteristics detected by coronary CT angiography and future coronary events. *J Cardiovasc Comput Tomogr.* 2013; 7(3):192–9. [PubMed: 23849492]

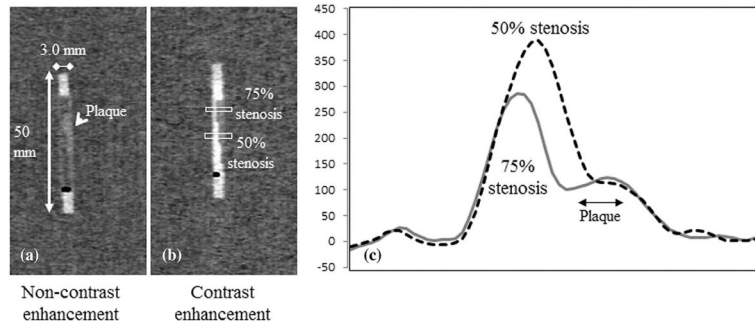


Figure 1. Multiplanar reformation (MPR) images with plaque on non-contrast (a) and contrast enhancement (b); CT voxel attenuation profile across the 50% and 75% plaques.

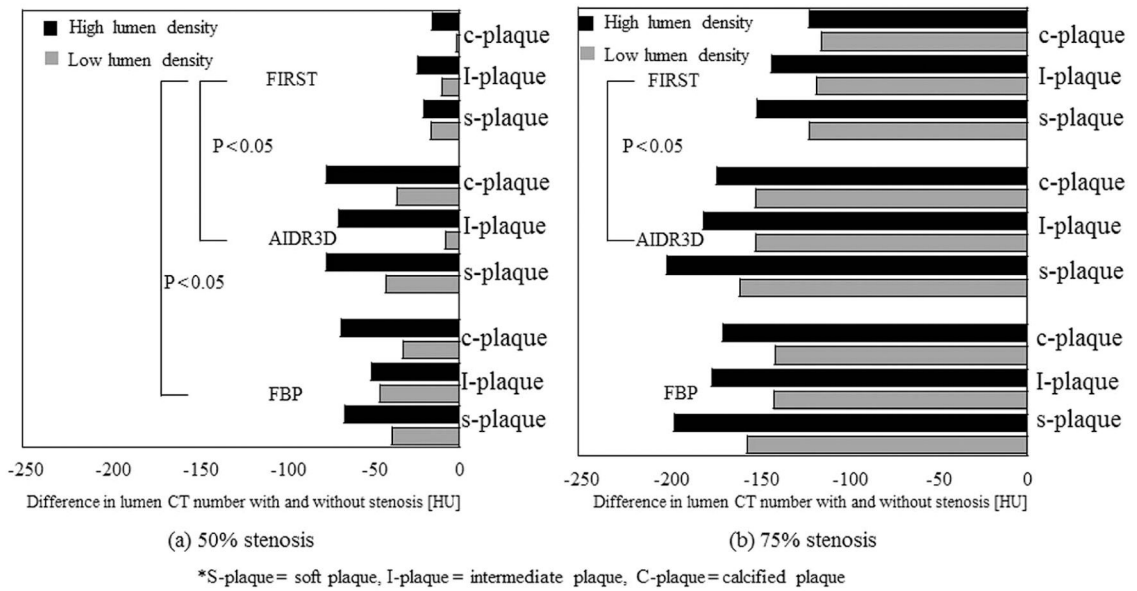


Figure 2. Difference in peak CT numbers with and without stenosis for FBP, AIDR3D, and FIRST at different plaque types and lumen densities, calculated from *peak lumen CT number without stenosis*–*peak lumen CT number with stenosis* [HU]. Figures (a) and (b) represent the cases with 50% and 75% stenosis, respectively.

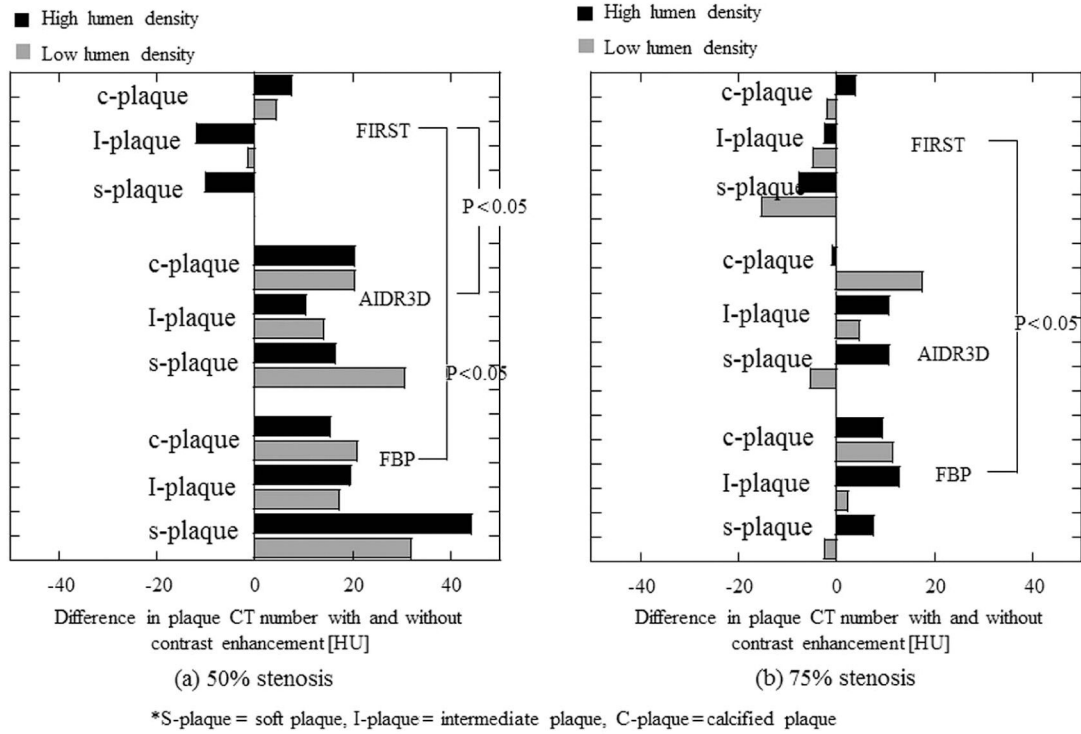


Figure 3. Difference in plaque CT numbers with and without contrast enhancement for FBP, AIDR3D, and FIRST at different plaque types and lumen densities, calculated from *plaque CT number without stenosis - plaque CT number with stenosis [HU]*. Figures (a) and (b) represent the cases with 50% and 75% stenosis, respectively.

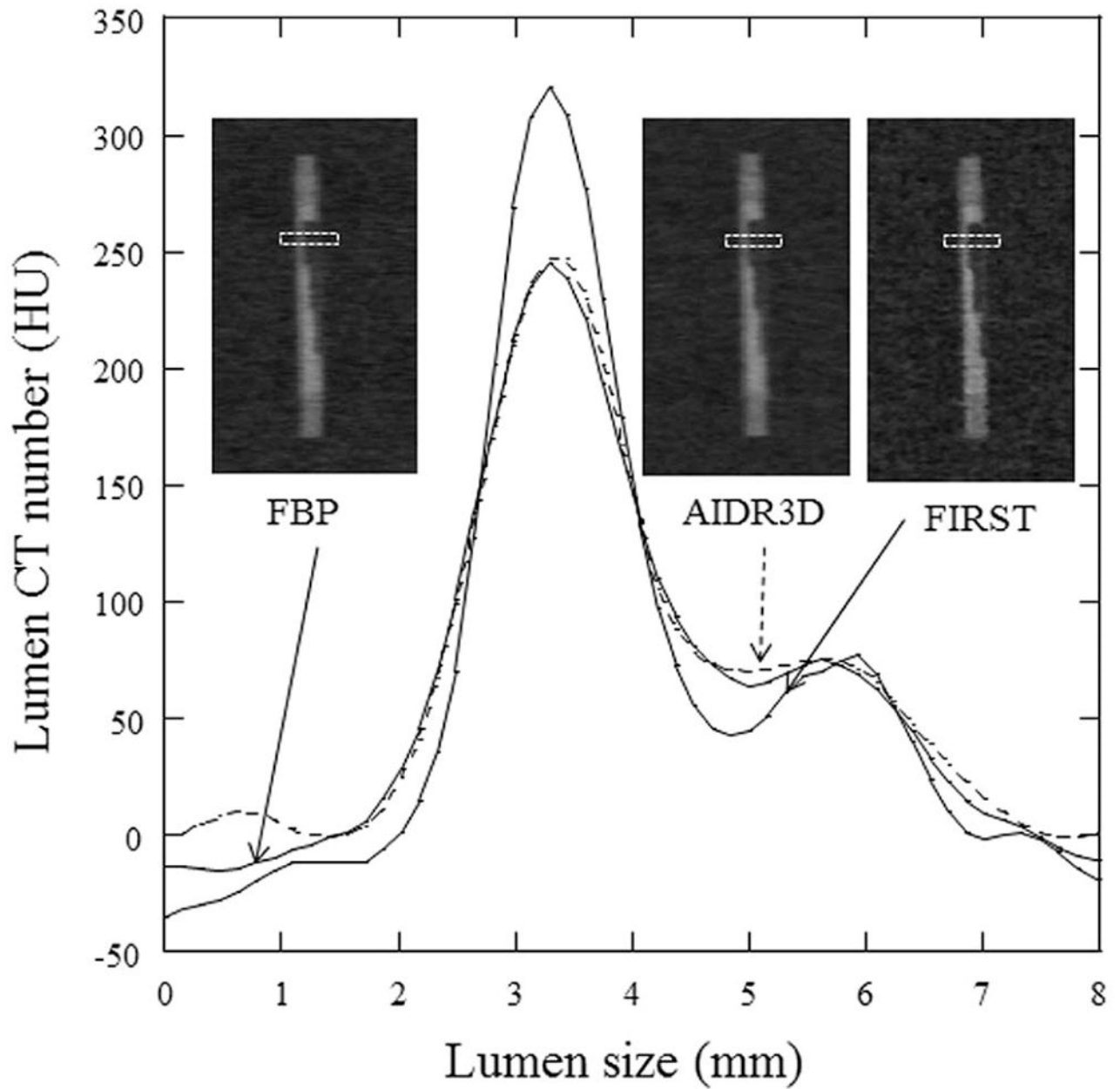


Figure 4. Profile curve for high lumen density including 75% stenosis of soft plaque with MPR images obtained at FBP, AIDR3D, and FIRST. The FIRST image gives a narrower profile curve than the other images.

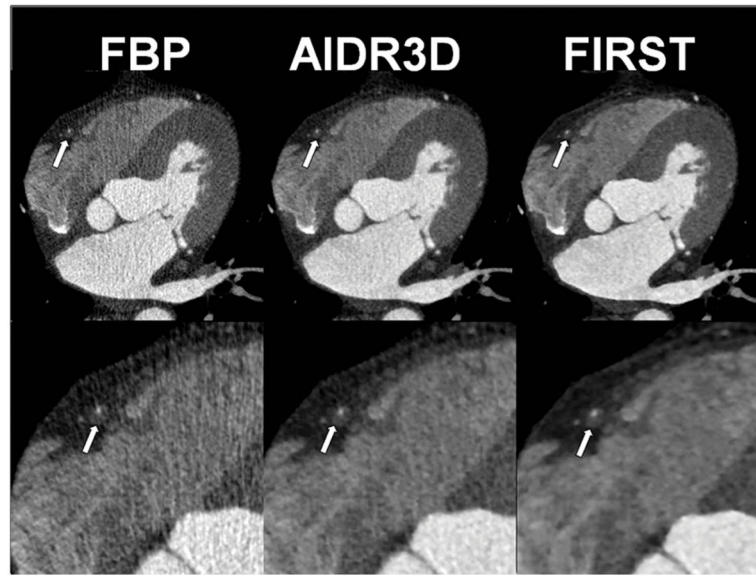


Figure 5. A 66-year-old man with chest pain. Non-calcified plaque is shown in the proximal right coronary artery (arrow). Clear margins of vessel lumen and plaque with less image noise are demonstrated on the FIRST image.

Table 1

Lumen CT number with and without stenosis for FBP, AIDR3D, and FIRST

	Lumen CT number without stenosis (HU)	Stenosis	Plaque type		
			S-plaque (HU)	I-plaque (HU)	C-plaque (HU)
FBP	370.5		331.8	325	338.8
	451.7		386.1	401.3	383.7
	370.4		328.2	362.5	335.2
AIDR3D	453.6	50%	377.2	384.5	377.2
	387.9		371.9	378.4	386.6
FIRST	464.7		444.7	441	449.6
<hr/>					
FBP	370.5		214.5	229.8	230
	451.7		255.4	276.3	282.3
	370.4		210	218.9	219.2
AIDR3D	453.6	75%	253.2	273.2	280.9
	387.9		266.6	270.6	273.4
FIRST	464.7		314	322.1	343.3

Table 2

Plaque CT number with and without contrast enhancement at 50% and 75% stenosis for FBP, AIDR3D, and FIRST

Stenosis	Plaque type	Plaque CT number without contrast enhancement (HU)	Plaque CT number with contrast enhancement (HU)	
			Low lumen density	High lumen density
FBP	s-plaque	48.2	80.2	92.4
	I-plaque	87.4	104.5	106.8
	c-plaque	152.2	173	167.6
50%	s-plaque	49.5	80	66
	I-plaque	89.4	103.7	99.6
	c-plaque	151.2	171.6	171.6
FIRST	s-plaque	50.1	50.2	40.2
	I-plaque	87.8	86.5	75.9
	c-plaque	148.5	153	156.1
FBP	s-plaque	50.1	47.7	57.7
	I-plaque	90.2	92.3	103
	c-plaque	158.2	169.6	167.6
75%	s-plaque	50.6	45.4	61.3
	I-plaque	91.6	96.3	102.1
	c-plaque	149.7	167.3	148.9
FIRST	s-plaque	49.8	34.5	41.9
	I-plaque	86.8	82.2	84.3
	c-plaque	150.3	148.5	154.2

* S-plaque= soft plaque, I-plaque= intermediate plaque, C-plaque=calcified plaque

Table 3

Ratio of lumen-plaque contrast in each method to that of FBP

Stenosis	Plaque type	Low lumen density			High lumen density		
		FBP	AIDR3D	FIRST	FBP	AIDR3D	FIRST
50%	s-plaque	1.0	1.0	1.3	1.0	1.1	1.4
	I-plaque	1.0	1.2	1.3	1.0	1.0	1.2
	c-plaque	1.0	1.0	1.4	1.0	1.0	1.4
75%	s-plaque	1.0	1.0	1.4	1.0	1.0	1.4
	I-plaque	1.0	0.9	1.4	1.0	1.0	1.4
	c-plaque	1.0	0.9	1.6	1.0	1.2	1.6

* S-plaque= soft plaque, I-plaque= intermediate plaque, C-plaque= calcified plaque Lumen-plaque contrast is calculated from subtraction of plaque CT number from peak lumen CT number.